COMPDYN 2015
5th ECCOMAS Thematic Conference on
Computational Methods in Structural Dynamics and Earthquake Engineering
M. Papadrakakis, V. Papadopoulos, V. Plevris (eds.)
Crete Island, Greece, 25–27 May 2015

EVALUATION OF THE APPLICABILITY OF THE LUGRE MODEL FOR MODELLING THE DYNAMIC BEHAVIOUR OF BOLT CONNECTED FRAMES

Sergio Sánchez Gómez[1], **Mihai I.Badila**[2], **Andrei Metrikine**[2]

[1]TU Delft
Faculty of Civil Engineering and Geosciences
Stevinweg1, 2628CNDelft, The Netherlands
e-mail: s.sanchezgomez, M.I.Badila, A.Metrikine@tudelft.nl

Keywords: Nonlinear dynamics, friction damping, LuGre model, Galerkin method.

Abstract. *In this paper the dynamics of a frame with bolted connections is studied both theoretically and experimentally. The connections are described using the Lund-Grenoble(LuGre) model. The problem of the dynamic response of the frame to a pulse load is studied using the Galerkin approach that reduces the governing equations to a set of nonlinear ODE's. They are latter solved numerically. It is shown that the theoretical predictions match the experimental observations well.*

1 Introduction

Nowadays buildings are becoming taller but also lighter and more slender. Those characteristics make buildings more sensitive to dynamic loads. Damping is an important but most uncertain parameter in the dynamic response of buildings under wind excitations. As a consequence, several researchers attempted to study it. Davenport [1] defined the main sources of energy dissipation in a tall building. Jeary [2] showed the relevance of the friction due to crack formation during high amplitude vibration and established a relation between damping and amplitude of vibration. Tamura [3] made significant improvements in damping prediction by developing practical models and applying data analysis methods [4], such as the random decrement technique to building measurements. Lagomarsino [5] developed a theoretical model to predict the friction damping in a building. However, he concluded that the model was not directly applicable. Because of the large amount of uncertainties in the damping prediction, developing a theoretical model to assess damping in buildings becomes very difficult. Only empirical formulas based on building measurements are available. All the mentioned researchers stated the importance of friction damping during high amplitude vibration scenarios in the damping prediction. The friction effects in a building can be very complex because they involve different phenomena that occur randomly such as the stribeck effect [6] and stiction effect [6] among others. The occurrence of these phenomena depends on many factors such as the construction material, the number of connected walls, the structural design of the building etc. The principal idea of this study is to find a general damping mechanism which captures the most important friction phenomena occurring in a building in high amplitude vibration scenarios. To this end, a friction damping mechanism called Lund-Grenoble(LuGre) model [7] is implemented. The details of this model are described in the following section. In order to get a better understanding of the LuGre mechanism a simple lab scale experiment has been carried out. In this paper an analytical approach to solve a case study applying the LuGre damping mechanism is presented. Moreover, the solutions of the model are compared with the lab scale experiment.

2 Model approach and governing equations

2.1 Model approach

Several damping mechanisms, ranging from linear viscous ones to complex combined mechanisms, are well described in literature [8, 9, 10]. Linear damping mechanisms are unlikely to predict damping in a high amplitude vibrations of buildings. This is because at high amplitudes the rubbing between contact surfaces produce friction. The friction damping has a nonlinear behaviour based on different phenomena (stribeck and stiction among others) that occur in an irregular manner. These phenomena make the magnitude of the friction change depending on the amplitude of vibration. Therefore, the focus on nonlinear mechanisms is necessary. Based on the goal of this study, the implementation of a single damping model to capture all the most important phenomena happening in a large amplitude vibration of buildings is needed. In consequence, the decision of using the LuGre model in this particular study was made. This decision is based on the fact that this is a general model that tackles the most relevant phenomena occurring when friction is present. The LuGre model was designed to deal with the friction between the surfaces of machine components. However, for this work an adaptation of this model in order to deal with friction in structural engineering problems is made. In this paper the LuGre model is applied to describe the dynamics of a frame structure. The results of the conducted study are compared with the data obtained from a lab scale experiment.

2.2 The LuGre model

In this section the LuGre model is presented in Eq. (1) and Figure (1). This model is an extension of the Dahl's model [6]. The Dahl's model, is a combination of the viscous model [11], Coulomb model [6] and the stiction model. However, the LuGre model, incorporates the bristle interpretation. The bristles represent the asperities at the microscopic level of the surfaces. This can be seen in Figure (1).

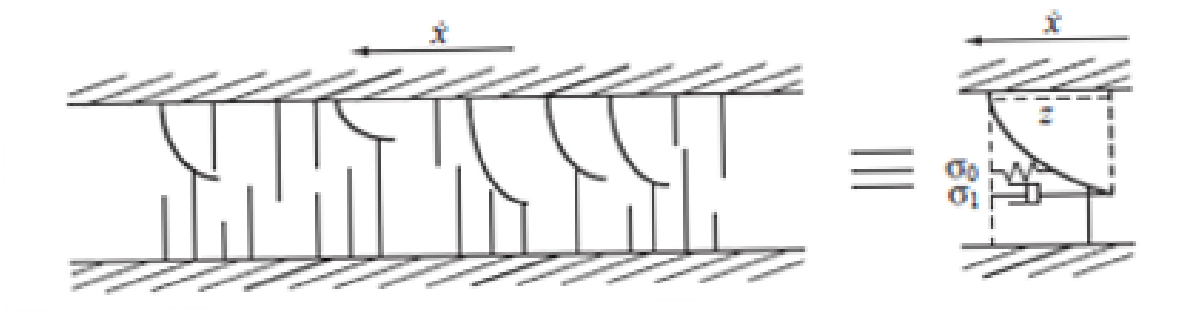

Figure 1: Bristle interpretation of the LuGre model

The LuGre model, is a combination of more simple damping models. This, also gives a very interesting point of view because with the simplification of the LuGre model, several other models are implicitly implemented.

$$
\begin{aligned}
F_L(v,z) &= \sigma_0 z + \sigma_1 \dot{z} + \sigma_2 \dot{x} \\
\dot{z} &= \dot{x} - \frac{\dot{x}}{g(\dot{x})} z \\
g(v) &= \frac{1}{\sigma_0}\Big(F_c + (F_s - F_c) e^{-\left(\frac{\dot{x}}{v_s}\right)^2}\Big)
\end{aligned} \tag{1}
$$

The LuGre model contains different parameters. Where F_L is the friction force, $\dot{x}$ is the relative sliding velocity at the friction interfaces, σ_0 is the bristle stiffness, σ_1 is the nonlinear damping coefficient, F_c is the Coulomb friction force, F_s is the stiction force, σ_2 is the linear viscous coefficient, and v_s is the stribeck velocity.

2.3 Case study

In this paragraph the application of the LuGre model in a case study is formulated and described below. The study consists in modeling a lab scale bolt connected steel frame. However, for simplification only one connection is taken into account. The model consists in a continuous Euler-Bernoulli beam [12] with a discrete element in its boundary as shown in Figure (2). The discrete element is composed by a translational spring and a friction mechanism. The friction damping mechanism is implemented using the LuGre model. In order to carry out the analytical nonlinear problem the Galerkin approach is employed.

2.3.1 Governing equations

The equation of motion and the boundary conditions for the model under consideration can be written in the following form(note that the LuGre element is accounted in the equation of motion):

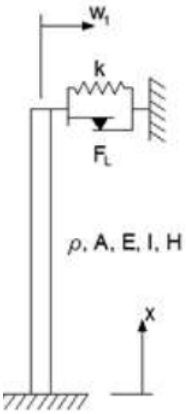

Figure 2: Physical interpretation of the model

$$
\begin{aligned}
EI\frac{\partial^4 w(x,t)}{\partial x^4} + \rho A\frac{\partial^2 w(x,t)}{\partial t^2} &= \delta(x-L)F(t) - \delta(x-L)F_L(\dot{w},\dot{z},z) \\
w(0,t) &= 0 \\
\frac{\partial w(0,t)}{\partial x} &= 0 \\
-EI\frac{\partial^2 w(H,t)}{\partial x^2} &= 0 \\
-EI\frac{\partial^3 w(H,t)}{\partial x^3} &= -kw(H,t)
\end{aligned} \tag{2}
$$

Where $w(x,t)$ is the beam deflection, E is the Youngs modulus, I is the moment of inertia of the cross sectional area, ρA is the inertial mass per unit of length, $\delta(x-L)$ is the Dirac delta function [13], $F(t)$ is the external load and $F_L(w,z,z)$ is the friction force.

The solution is assumed to be in the following form:

$$
w(x,t) = \sum_{n=1}^{\infty} W_n(x)q_n(t) \tag{3}
$$

Where $W_n(x)$ are the eigenfunctions that satisfy the boundary conditions and $q_n(t)$ are the unknown time dependent functions. Substituting Eq. (3) into the equation of motion and making use of the orthogonality condition, the Galerkin projection is formulated.

$$
\begin{aligned}
&\int_0^H \Big(EI\sum_{n=1}^{\infty} W_n''''(x)q_n(t) + \rho A\sum_{n=1}^{\infty} W_n(x)\ddot{q}_n(t)\Big)W_n(x)dx = \\
&\int_0^H \Big(\delta(x-L)F(t) - \delta(x-L)F_L(\sum_{n=1}^{\infty} W_m(x)\dot{q}_m(t),\dot{z},z)\Big)W_n(x)dx
\end{aligned} \tag{4}
$$

2.3.2 Evaluation of the natural frequencies and eigenfucntions

First, the eigenfunctions $W_n(x)$ should be determined before the solution can be carried out. The modes are calculated using the following equation of motion

$$EI\frac{\partial^4 w(x,t)}{\partial x^4} + \rho A\frac{\partial^2 w(x,t)}{\partial t^2} = 0 \tag{5}$$

and the boundary conditions given in Eq. (2). The physical representation of such a system is as shown in Figure (3).

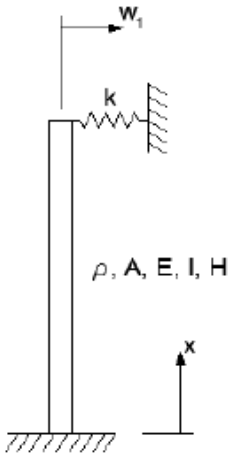

Figure 3: Model without the non-linear components

Note that the friction damping mechanism and the input force are not included in the Eq. (5), but they are accounted as a part of the equation of motion in Eq. (2). This enables to use the Galerkin approach. The solution of Eq. (5) is assumed as:

$$w(x,t) = W(x)cos(wt + \phi) \tag{6}$$

Substituting Eq. (6) into Eq. (5) the eigenvalue problem can be formulated.

$$W''''(x) - \beta^4 W(x) = 0 \tag{7}$$

where $\beta^4 = \frac{\lambda^2 \rho A}{EI}$ and the general solution for $W(x)$ is:

$$W(x) = C_1 e^{\beta x} + C_2 e^{-\beta x} + C_3 e^{i\beta x} + C_4 e^{-i\beta x} \tag{8}$$

inserting the general solution into the boundary conditions of Eq. (2), the natural frequencies and the mode shapes can be obtained:

$$\begin{pmatrix} 1 & 0 & 1 & 0 \\ 0 & 1 & 0 & 1 \\ cosh(\beta H) & sinh(\beta H) & -cos(\beta H) & -sin(\beta H) \\ (H\beta)^3 sinh\beta H - \frac{H^3 k}{EI} cosh(\beta H) & (H\beta)^3 cosh\beta H - \frac{H^3 k}{EI} sinh(\beta H) & (H\beta)^3 sin\beta H - \frac{H^3 k}{EI} cos(\beta H) & -(H\beta)^3 cos\beta H + \frac{H^3 k}{EI} sin(\beta H) \end{pmatrix} \begin{pmatrix} C_1 \\ C_2 \\ C_3 \\ C_4 \end{pmatrix} = 0$$

Now, by setting to zero the determinant the natural frequencies can be determined.

$$\mathbf{det}(\beta) = 0 \tag{9}$$

The eigenfunciton of the system can be obtained after the determination of the coefficients C_i.

$$W(x) = cosh(\beta_n x) - cos(\beta_n x) - \frac{cosh(\beta_n H) + cos(\beta_n H)}{sinh(\beta_n H) + sin(\beta_n H)}(sinh(\beta_n x) - sin(\beta_n x)) \tag{10}$$

2.3.3 Application of the Galerkin method

Once the natural frequencies and eigenfunctions are determined, the solution of the complete system can be carried out. Note that on the right hand side of Eq. (2) the Dirac delta function is presented. Therefore, in order to work out the right hand side of the equation a property of the Dirac delta function is applied [13].

$$\int_{-\infty}^{\infty} \Big(\delta(x-L)F_L(\sum_{m=1}^{\infty} W_m(x)\dot{q}_m(t), \dot{z}_n, z_n)\Big)W_n(x)dx = F_L(\sum_{m=1}^{\infty} W_m(H)\dot{q}_m(t), \dot{z}_n, z_n)\Big)W_n(H) \tag{11}$$

this leads to:

$$(\lambda_n^2 q_n(t) + \ddot{q}_n(t)\Big)\rho A\int_0^H W_n^2(x)dx = F(t)W_n(H) - F_L(\sum_{m=1}^{\infty} W_m(H)\dot{q}_m(t), \dot{z}_n, z_n)\Big)W_n(H) \tag{12}$$

Finally a set of equation can be formulated as.

$$\begin{aligned} \dot{q}_n &= v_n \\ \dot{v}_n &= \frac{F(t)W_n(H) - F_L(\sum_{m=1}^{\infty} W_m(H)\dot{q}_m(t), \dot{z}_n, z_n\Big)W_n(H)}{A_n} - \lambda_n^2 q_n(t) \\ \dot{z}_n &= \dot{v}_n - \frac{\dot{v}_n}{g(\dot{v}_n)}z_n \end{aligned} \tag{13}$$

where:

$$A_n = \rho A\int_0^H W_n^2(x)dx \tag{14}$$

A numerical method is used in order to solve this system of ordinary differential equations. The procedure is repeated adding modes until the system converges in order to find a sufficiently accurate solution.

3 Experimental set up

In this section the experimental set up is presented. It consists of three steel beams with the following dimensions 1x0.1x0.01m. The beams are connected forming a frame shape; the vertical beams are assumed to be fully clamped. The horizontal beam is bolted through a square connection to the vertical beams (Figure (4)). Therefore, we force the system to generate more friction due to a larger friction surface. In this experiment several tests were performed. In order to excite the structure a hammer with a force transmitter was used to introduce an impulse signal to the structure.

Figure 4: Experiment set up

First, the response of the structure was measured using a fully tight connection. The response of the system, measured from the accelerometer closer to the connection can be noted from Figure (5a). Second, the influence of the loosen connection was tested. Therefore, the lower bolts of the connection were loose and subsequently hand tightened. In consequence, higher friction and hence, higher damping was measured with the same accelerometer. This can be noted comparing the decay signal of Figure (5a) with Figure (5b).

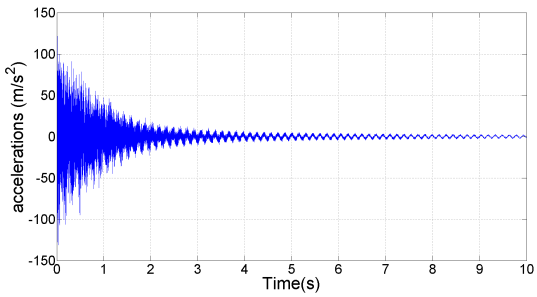

(a) Response signal of the structure with the fully tight connection

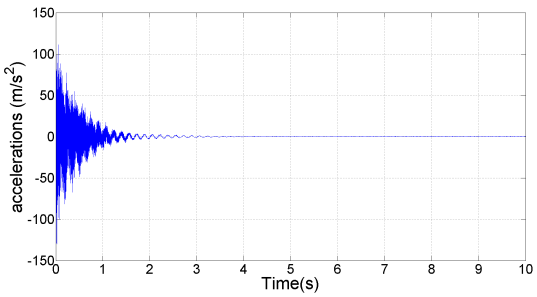

(b) Response signal of the structure with loosen bolts

Figure 5: Measured signals

Finally, filtering the signal of test with the loosen connection it can be noted how nonlinearities appear in the system (Figure (6)).

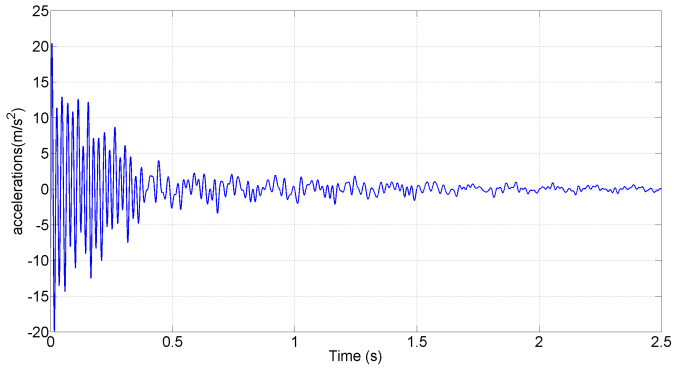

Figure 6: Filtered signal of the loosen bolts test

4 Results

The procedure proposed above (section 2) is used in this section to present the results of the study. The natural frequencies and the responses of the model are compared with the measurements from the experiment. Moreover, the sensibility study of the model parameters is presented. Although this is not a comprehensive analysis, several conclusions can be elucidated from studying how the parameters of the model influence the dynamic behaviour of the system. The properties of the system are described in Table (1).

Material properties		
Young modulus (E)	200e9	$\frac{N}{m^2}$
Density (ρ)	7850	$\frac{kg}{m^3}$
Geomerty		
Lenght (L)	1	m
Width (b)	0.1	m
Thickness (t)	0.01	m

Table 1: Material properties and geomerty

4.1 Natural frequencies and mode shapes

According to the procedure described in section 2.3.2. The modes are approximated by setting the non-linear parts to zero. This means that the natural frequencies and the mode shapes are determined using Eq. (5) and the boundary conditions described in Eq. (2). The experimental data obtained in the test with the fully tight connection (Figure (5a)) is used to compare it with the approximated natural frequencies obtained with the model(Figure (7a)).

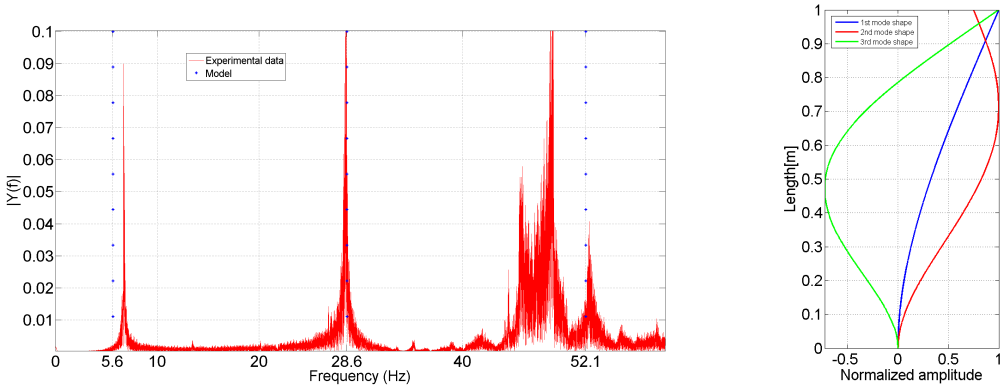

Figure 7: a) Modes of the model and the measurement; b) Model mode shapes

The stiffness of the attached spring is very difficult to determine experimentally. Therefore, it is tuned in order to match the natural frequencies of the experimental result of the fully tight connection test. As a result can be seen how the natural frequencies of the model match the results obtained from the experimental data.

4.2 The system response

Once the modes are found the system can be evaluated by using Eq. (2). Therefore the friction element and the input force are taken into account. The LuGre mechanism contains several parameters as described in section 2.2. This means that the influence of these parameters can be determined.

4.2.1 The influence of the LuGre parameters

The influence of the LuGre parameters is examined in the following figures.

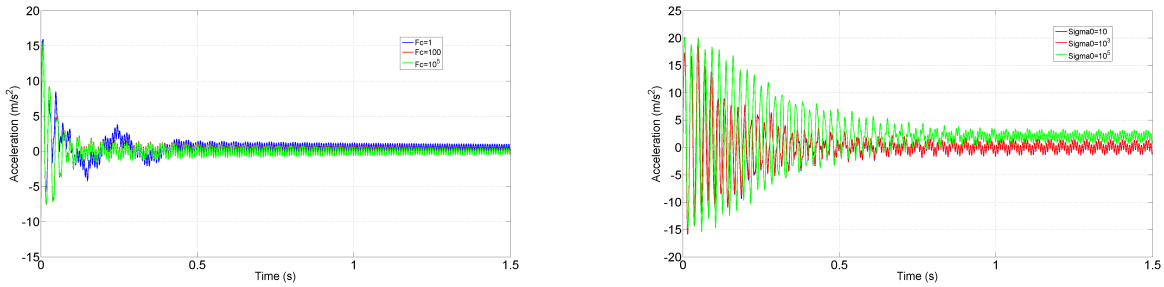

(a) Coulomb friction

(b) Bristles stiffness

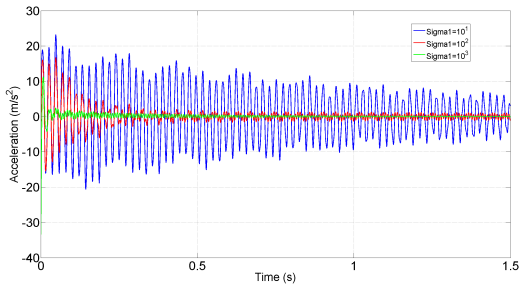

(c) Bristles damping

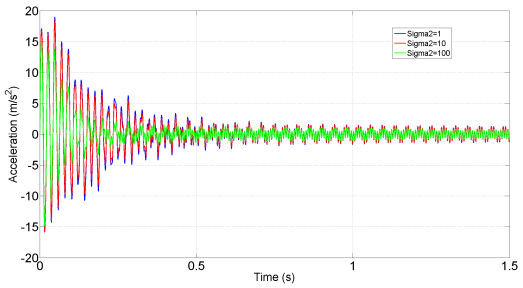

(d) Overall viscous damping

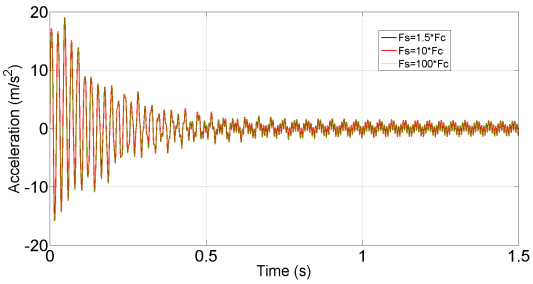

(e) Stiction force

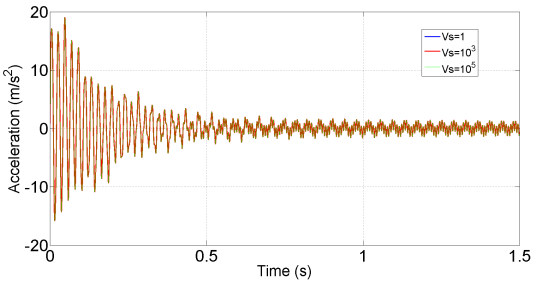

(f) Stribeck velocity

Figure 10: LuGre parameters interpretation

From Figure (10a) it can be seen that the Coulomb friction is a parameter with a high influence on the performance of the friction damping. As occurred with the Coulomb friction the stiffness of the bristles σ_0 has a high influence on the total damping of the system(Figure (10b)). Moreover, the damping coefficient of the bristles σ_1 has a very important influence on the decay (Figure (10c)). The damping of the overall system has a large influence in the decay of the system as can be noted from Figure (10d). The effects of the stiction force are shown in Figure (10e). It can be noted that the influence of the stiction force is negligible. The final examined parameter is the stribeck velocity. This parameter has a little influence on the performance of the system as can be noted from Figure (10f).

As a consequence of the parameters examination, the parametrization of the model can be performed. Therefore, the following table contains a range of values suitable to match the case study.

σ_0	σ_1	σ_2	F_c	F_s	v_s
$10^{1.8}$	$10^{1.8}$	0.001	1	1.5	0.001

Table 2: LuGre parameters

A value for the different parameters has been selected in order to reproduce the output obtained from the lab scale experiment. The model results in comparison with the experimental data can be noted in Figure (11).

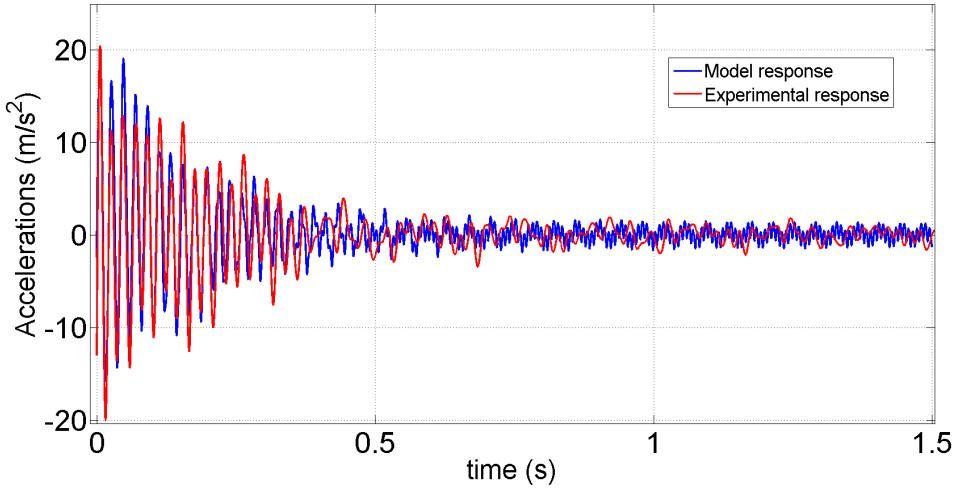

Figure 11: Comparison of the time domain response of the model and the experiment

From Figure (12), it can be seen that the results of the model match relatively well with the results obtained in the experiment.

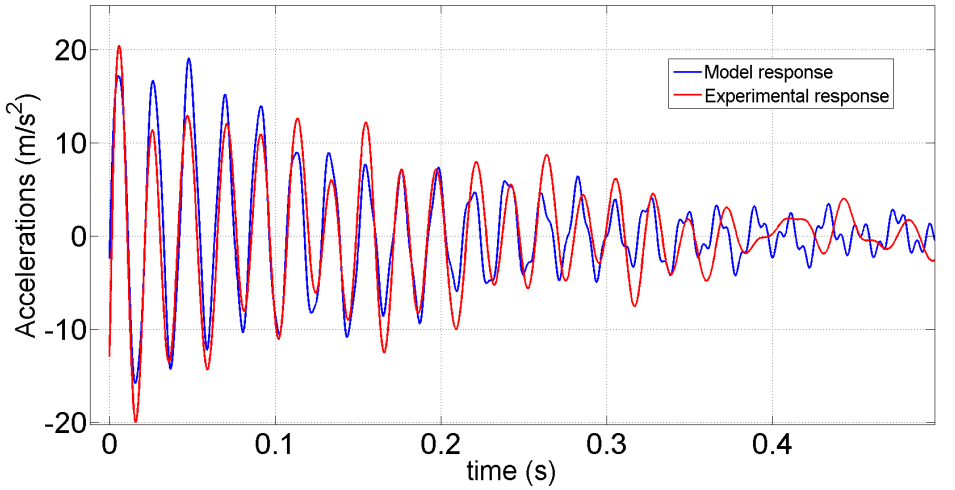

Figure 12: Detailed observation of the time domain response of the model and the experiment

5 Conclusions

In this paper, an analysis of the implementation and parameterization of the LuGre model has been accomplished. For this purpose, a case study which reproduces as accurately as possible, the response of a lab scale bolt structure has been performed. The reproduction of this experiment is performed using the LuGre model included as a boundary condition of an Euler-Bernoulli beam. In further research this model will be used in order to capture the response of another type of connections. The purpose is to use a single model, in this case the LuGre model in order to capture the friction-associated dissipation in a wide spectrum of conditions.

REFERENCES

[1] A.G. Davenport and P. Hill Caroll, Damping in tall buildings: its variability and treatment in design; *American Society of Civil Engineers (ASCE) (*1986*).*

[2] A.P. Jeary, Damping in tall buildings. A mechanism and a predictor; *Earth. Eng. Struct. Dyn, (*1986*)* $733 - 750$.

[3] Y. Tamura, N. Satake, T. Arakawa, A. Sasaki, Damping evaluation using full-scale data of buildings in Japan; *Journal of structural engineering.*

[4] J.C. Asmussen, Modal analysis based on the Randon Decrement technique-Applications to civil engineering structures; *Aalborg University, Denmark (*1997*).*

[5] S. Lagomarsino, Forecast models for damping and vibration poriods of buildings; *Wind Engineering and Industrial Aerodynamics, (*1993*).*

[6] V. van Geffen, A study of friction models and friction compensation; *Technische Universiteit Eindhoven (*2009*).*

[7] C. Canudas de Wit, H. Olsson, J.Åström, A new model for control of system with friciton; *IEEE transactions on automatic control. VOL* 40*. No* 3*, march* 1995.

[8] W.W. Soroka, Note on the relations between viscous and structural damping coefficients; *J. aeronaut. sci.* 16*,* $409 - 410$ *and* 448 *(*1949*).*

[9] D.E. Hudson, Equivalent viscous friction for hysteretic systems with earthquake-like excitations; *Proc. 3rd world conf earthquake* 12 *eng. Auckland and Wellington,* 11*,* 185-201 *(*1965*).*

[10] L.S. Jacobsen, Damping in composite structures; *Proc.* 2*nd world conf earthquake eng. Tokyo and Kyoto,* 1029-1044 *(*1965*).*

[11] S. adhikari AND J. Woodhouse, Identification of damping:Part 1, viscous damping; *Journal of Sound and vibration (*2001*)* 243*(*1*),* 43-61.

[12] J.M.J. Spijkers, A.W.C.M. Vrouwenvelder, E.C. Klaver, Dynamics of StructuresCT4140-Part 1-Vibrations of Structures; *Faculty of Civil Engineering and Geosciences Section of Structural Mechanics, Delft University of Technology.*

[13] J. Sethuraman, Dirac delta function and some of its applications; *Vinayaka Missions Kirupananda Variyar Engineering college.*